Synthesis and characterization of highly dispersed molybdenum species in SBA-15 mesoporous molecular sieves

Emmanuel Briot,*[a] Jean-Yves Piquemal[b] and Jean-Marie Brégeault[a]

[a] *Systèmes Interfaciaux à l'Echelle Nanométrique (CNRS FRE 2312), Université Pierre et Marie Curie, Case 196, 4 place Jussieu, 75252, Paris Cedex 05, France. E-mail: briot@ccr.jussieu.fr*

[b] *Laboratoire de Chimie des Matériaux Divisés et Catalyse - ITODYS, Université Denis Diderot, Case 7090, 2 place Jussieu, 75251, Paris Cedex 05, France*

Received (in Montpellier, France) 4th February 2002, Accepted 27th May 2002
First published as an Advance Article on the web 9th September 2002

An original pathway involving H_2O_2 is described for the incorporation of highly dispersed molybdenum oxo species into the mesoporous network of an SBA-15 type silica. This procedure requires a mixture of templating agents: the triblock copolymer $EO_{20}PO_{70}EO_{20}$ and the quaternary ammonium salt CTMACl, which are commonly used for SBA-15 and MCM-41 syntheses, respectively. Physicochemical techniques clearly demonstrate that the triblock surfactant/CTMACl molar ratio has to be carefully controlled in order to *i*) obtain a significant amount of Mo in the mesoporous silica and *ii*) retain the SBA-15 structure.

1. Introduction

The development of new heterogeneous catalysts or the heterogenization of homogeneous systems for catalytic processes is a highly attractive topic in current chemical research.[1,2] Among oxidation reactions, in particular, olefin epoxidation has been intensively studied since epoxides are very important intermediates in many industrial processes. Transition metals such as Mo, W, Re, Ti, Mn, Ag, *etc.* are well known to catalyse epoxidation. In the early 1990s, mesoporous silica molecular sieves were developed.[3–5] One of them, called MCM-41, has a hexagonal structure with uniform pore size in the 20–100 Å range. These discoveries have raised novel possibilities for preparing transition metal-containing materials by capillary impregnation, grafting or insertion. Some of these methods require expensive organometallic precursors (*e.g.* alkoxides) and lead to an interaction between the transition metal and the mesoporous solid surface which is weak and can facilitate the leaching of active species.

We have recently described a novel way, the so-called peroxo route, for inserting transition metals (*i.e.* Mo, W, Re) into MCM-41 with a Si/M ratio as low as *ca.* 30 and a high metal dispersion, using a sol–gel process in an acidic medium ($H_2O/H_3O^+/H_2O_2$) at room temperature under atmospheric pressure.[6–8] Several low-condensed neutral or anionic oxoperoxometalate species are generated at pH 1–2 in the presence of excess H_2O_2,[9,10] avoiding the formation of oligomeric species[6–8] such as the Keggin units (*i.e.* $[SiM_{12}O_{40}]^{4-}$, M = Mo, W),[11–13] which obviously do not favour high dispersion of the metal in mesoporous molecular sieves. On the contrary, all syntheses performed in an acidic medium without hydrogen peroxide, denoted the oxo route, lead to the formation of large iso- (or hetero-) polyoxometalates[6–8] and the calcination of native materials leads to segregated solids (MO_3 + silica; M = Mo, W).

Preliminary catalysis tests ((*R*)-(+)-limonene,[7] cyclooctene epoxidation[6]) showed that leaching cannot be avoided with MO_x-MCM-41 materials, probably due to imperfect crystallization of the solid and to the nucleophilicity of the liquid reactants (H_2O_2, *t*-BuOOH, *etc.*).

Recently, Stucky *et al.*[14,15] described the synthesis of a new class of mesoporous materials, denoted SBA-*n*, which display excellent interfacial stability. In the present paper, the peroxo route for inserting transition metals in mesoporous materials has been extended successfully to the synthesis of Mo-SBA-15.

2. Experimental

2.1. Materials

Tetraethyl orthosilicate (TEOS) (purum 99%), cetyltrimethylammonium chloride (CTMACl) (25 wt.% in water), cetyltrimethylammonium bromide (CTMABr) ($\geqslant$99%) and MoO_3 (purum, 99.5%) were purchased from Fluka. The poly(ethylene glycol)-*block*-poly(propylene glycol)-*block*-poly(ethylene glycol), average M_n *ca.* 5800, *ca.* 30 wt.% ethylene glycol (triblock copolymer, $EO_{20}PO_{70}EO_{20}$) was purchased from Aldrich. K_2MoO_4 and aqueous H_2O_2 (30 wt.%) were purchased from Prolabo, aqueous HCl (37 wt.%; 12.5 M) from Carlo Erba.

2.2. Syntheses

A typical synthesis (peroxo route) was adapted from the method previously described.[6–8,14,15] In solution A, $EO_{20}PO_{70}EO_{20}$ (4 g), H_2O (137 mL), 37% HCl (20 mL) and the desired amount of CTMACl are stirred at room temperature until the surfactants are completely dissolved. In solution B, MoO_3 (118 mg), H_2O (2.5 mL) and 30% H_2O_2 (2.5 mL) are reacted at 60 °C to generate a yellow solution of low-condensed oxo-peroxo species (mainly $[MoO(O_2)_2(H_2O)_2]$ and $[O\{MoO(O_2)_2(H_2O)\}_2]^{2-}$). TEOS (9.1 mL) is added to solution A; solution B (cooled at room temperature) is then mixed once gel formation has set in. The molar composition of the synthesis gel (for sample D, see Table 1) is: 1 TEOS/0.01 CTMACl/0.02 $EO_{20}PO_{70}EO_{20}$/5.9 HCl/0.6 H_2O_2/0.02 Mo(VI)/205 H_2O. Note that in all syntheses, the amount of $EO_{20}PO_{70}EO_{20}$ was kept constant. The resulting gel is aged for 4 h with moderate stirring at room temperature. The yellow solid is then suction filtered, washed with a large amount of distilled water (2 × 100 mL) and dried overnight. The white native sample is

Table 1 Elemental analyses data and surfactant molar ratio used in the synthesis

Samples	$EO_{20}PO_{70}EO_{20}$/ CTMACl (molar ratio)	Mo (wt.%)$_{exp}$ [a]	$(Si/Mo)_{exp}$ [b] (molar ratio)
A	0.25	3.49	41
B	0.5	2.97	46
C	1	2.45	58
D	2	1.09	137
E	4	0.42	356
F	∞	0.30	500

Reaction time was 4 hours at room temperature for all samples.[a] Analyses of the calcined materials. [b] The molar ratio $(Si/Mo)_{initial}$ of the gel is 50 for all samples.

calcined in air (200 cm^3 min^{-1}, 1 K min^{-1}) from ambient to 773 K (samples maintained at the final temperature for 6 h) to remove the template.

A molybdenum-containing MCM-41 material was also synthesized by the oxo route, following the method previously described.[7,16] To a solution containing CTMABr (7.29 g) and 37% HCl (8 mL) in H_2O (270 mL), were added the transition metal precursor, K_2MoO_4 (0.48 g) and TEOS (22.3 mL). After stirring at room temperature for 24 h, the yellow solid was recovered by filtration and treated as described above.

2.3. Physicochemical techniques

X-ray diffraction patterns were recorded on an INEL XRG3000 diffractometer (Cu-Kα radiation) using a curved detector from 0.6 to 13° (2θ) with a resolution of 0.03° (counting time: 10 min). The powdered samples were mounted in capillaries (Lindeman tubes) and the diffractometer was calibrated using a standard sample (silver behenate, $(C_{22}H_{43}O_2)Ag$, Alfa). Adsorption and desorption isotherms for nitrogen were obtained at 77 K using a Micromeritics ASAP 2010. The samples were outgassed at 393 K and 0.1 Pa for 12 h before measurements. Specific surface area values were obtained using the BET (Brunauer–Emmett–Teller) equation; the mean pore size diameters are those of the BJH (Barrett–Joyner–Halenda) method,[17] with the desorption branch being analysed, using the Harkins–Jura model for the statistical film thickness (*i.e.* $t = [13.99/(0.034 - \log P/P_0)]^{0.5}$). Although the BJH method is usually considered to underestimate the real pore size values,[18] it can nevertheless be used for a comparative estimation of the pore size distribution. Elemental analyses were carried out at the Service Central d'Analyse (CNRS-Lyon) by ICP-AES (Inductively Coupled Plasma–Atomic Emission Spectroscopy) after alkaline fusion with $Li_2B_4O_7$. TEM (Transmission Electron Microscopy) and EDX (Energy Dispersive X-ray Analysis) were performed using a Link AN10000 system (Si–Li diode detector) connected to a JEOL JEM 100 CXII transmission electron microscope operating at 100 kV and equipped with an ASID 4D scanning device (STEM mode). The X-rays ($SiK_{\alpha 2}$ and MoL_1 lines) emitted from the specimen upon electron impact from rectangular domains (*e.g.* 150×200 nm^2) were collected in the 0–20 keV range for 250 s. UV-visible diffuse reflectance spectroscopy was performed on a Varian Cary 5E spectrophotometer equipped with an integration sphere and coupled to a microcomputer.

3. Results and discussion

3.1. Elemental analysis

The molar ratio of the templates (*i.e.* $EO_{20}PO_{70}EO_{20}$/CTMACl) and elemental analysis data are reported in Table 1. Obviously, the presence of the neutral surfactant alone does not allow significant molybdenum incorporation (see Table 1, sample F). Moreover, the $EO_{20}PO_{70}EO_{20}$/CTMACl ratio is an important parameter which must be adjusted to obtain, in the calcined materials, a molar ratio $(Si/Mo)_{exp}$ in accordance with the initial value of the gel (*i.e.* 50). Except for samples E and F, molybdenum incorporation increases linearly with the amount of CTMACl, as can be seen in Fig. 1. The optimum is reached with sample B for a $EO_{20}PO_{70}EO_{20}$/CTMACl ratio of about 0.5 to prepare a hexagonal SBA-15 mesostructure. For lower values, such as 0.25, there is significant incorporation of molybdenum with $(Si/Mo)_{exp} = 41$, but the resulting material is disorganized and no longer shows the SBA-15 structure (*vide infra*).

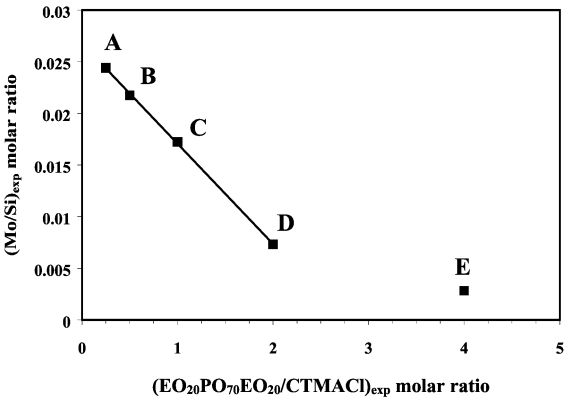

Fig. 1 $(Mo/Si)_{exp}$ molar ratio as a function of the $(EO_{20}PO_{70}EO_{20}/CTMACl)_{exp}$ molar ratio.

3.2. XRD, TEM, EDX and nitrogen adsorption

The X-ray diffraction pattern (Fig. 2b) of sample B displays only one large peak at very low angle (2θ = 1.1°) which can be indexed as (100), indicating that the nearly amorphous hexagonal structure of SBA-15 is characterized by short-range order. Crystallinity should be increased by using hydrothermal synthesis (100 °C at autogeneous pressure), which is well known to promote the maturation of mesoporous materials.[19] However, the presence of peroxo species prohibits the use of hydrothermal treatment during the early stages of the synthesis. Based on hexagonal symmetry, the unit cell parameter a_0 can be calculated using the formula: $a_0 = 2d_{100}/\sqrt{3}$. All samples have similar X-ray patterns, except for sample A which displays a very broad low-angle peak (Fig. 2a).

Further evidence for a hexagonal mesostructure is provided by the TEM images presented in Fig. 3a and b. The

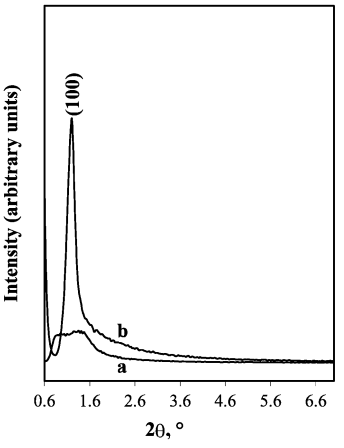

Fig. 2 X-Ray diffraction patterns of sample A (a) and sample B (b).

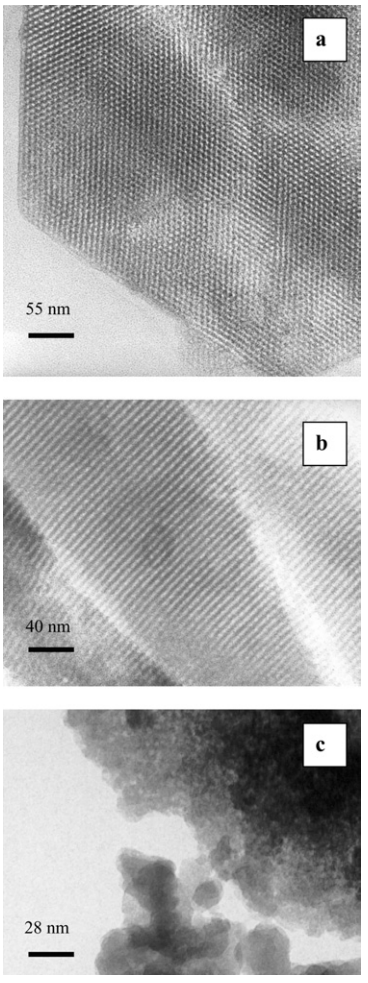

Fig. 3 TEM micrographs of sample B with the electron beam (a) parallel to the pore axis, (b) perpendicular to the pore axis; (c) TEM of sample A.

micrographs show well-defined mesoporous structures, suggesting a hexagonal arrangement of the mesophase. On the contrary, sample A exhibits a worm-like structure with a disorganized porous network (see Fig. 3c).

Table 2 gives the parameters obtained from nitrogen adsorption and X-ray diffraction. Samples B to F exhibit similar nitrogen adsorption–desorption isotherms, characteristic of mesoporous solids (*i.e.* type IV isotherms with a hysteresis loop, see Fig. 4b). The BJH pore size distribution (Fig. 5b) shows only one mean pore diameter (*ca.* 37 Å), indicating that the porosity of the materials can be assigned to SBA-15 alone, and not to a mixture of SBA-15 and MCM-41. For sample A (Fig. 4a), the nitrogen adsorption–desorption isotherm is characteristic of MCM-41 type materials (*i.e.* type IV isotherm with no hysteresis). However, the pore size distribution is much

Table 2 Mean pore diameter (dp), wall thickness (w), specific surface area (S_{BET}) and unit cell parameter (a_0) obtained from nitrogen adsorption isotherms and X-ray diffraction patterns

Samples	$S_{BET}/m^2\ g^{-1}$	a_0/Å	dp/Å	w^a/Å
A	947 ± 2	—	22	—
B	911 ± 7	85	37	48
C	935 ± 8	93	37	56
D	989 ± 9	93	37	56
E	967 ± 8	90	37	53
F	844 ± 7	90	37	53

[a] $w = a_0 - dp$.

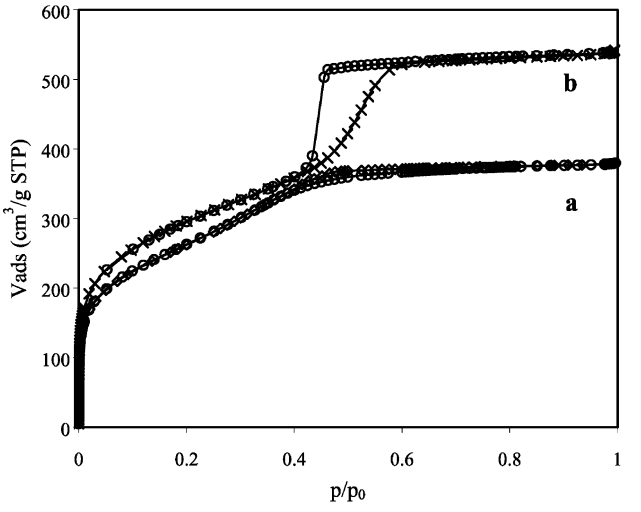

Fig. 4 Nitrogen adsorption–desorption isotherms of sample A (a) and sample B (b).

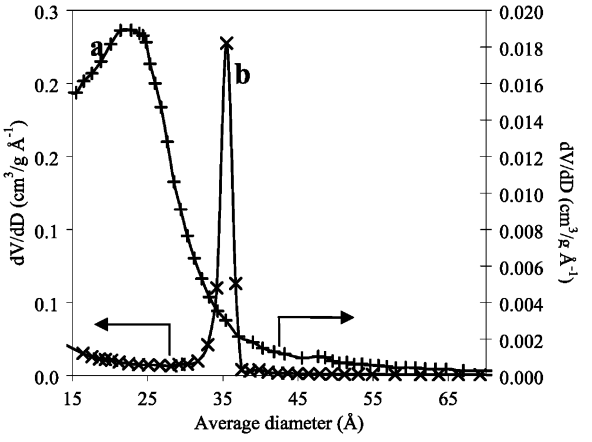

Fig. 5 Pore size distributions (BJH method using the desorption branch) of sample A (a) and sample B (b).

broader for sample A than for samples B to F, with a reasonably well-defined maximum near 22 Å (see Fig. 5a), indicative of a lower structural ordering of the material.

Except for sample A, the SBA-15 structure is preserved over a wide range of $EO_{20}PO_{70}EO_{20}$/CTMACl ratios, indicating that the triblock surfactant acts alone as the template. Molybdenum incorporation can be mainly explained by ion-pairing effects involving the cationic $CTMA^+$, the anionic peroxo species and (protonated) silanols (see Scheme 1). However, neutral peroxo species, $[MoO(O_2)_2(H_2O)_2]$, can also be involved

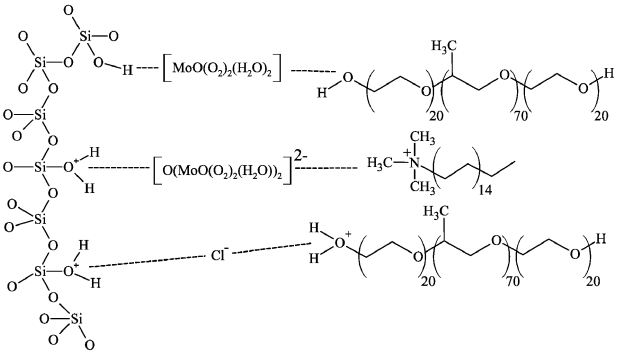

Scheme 1 Proposed interactions occurring during the synthesis of Mo-SBA-15.

Table 3 EDX data for sample B

Area	Si (% at.)	Mo (% at.)	(Si/Mo) (mol/mol)
1	97.3	2.7	36
2	97.9	2.1	46
3	97.7	2.3	42
4	98.0	2.0	50
5	97.4	2.6	38
6	97.2	2.8	35
7	97.9	2.1	46
8	97.9	2.1	46
9	98.1	1.9	51
10	98.2	1.8	53
11	98.0	2.0	48
12	98.2	1.8	53
Average (SD)	—	—	45 (6.3)
Elemental analysis	—	—	46

to a slight extent, as confirmed by sample F which contains Mo ($(Si/Mo)_{exp} = 500$) although no $CTMA^+$ was used in the synthesis.

EDX analyses (Table 3) indicate that the average (Si/Mo) value is very close to the elemental analysis results (*i.e.* 46), whatever the location of the X-ray beam on the sample. Moreover, the standard deviation (SD = 6.3) is very low compared to the results obtained with Mo-MCM-41 materials (SD = 29.0 and 75.9 for samples prepared by the peroxo and oxo routes, respectively[7]). These data clearly demonstrate that the peroxo route can be used to obtain a very high dispersion of molybdenum within the mesoporous network of SBA-15.

So far, all these results indicate that the peroxo route can be applied to the synthesis of Mo-SBA-15, with a mixture of organic templates, leading to a well-defined, single-mean pore diameter material with a high dispersion of the molybdenum centres.

3.3. UV-visible diffuse reflectance spectroscopy

The spectra of thermally treated mesoporous materials usually display broad absorption bands of high-energy maxima. The spectra of Mo-SBA-15 and Mo-MCM-41 obtained with the peroxo route are similar (Fig. 6). These results confirm the presence of low-nuclearity molybdenum oxo species inserted into the silica framework, if the synthesis is performed by the peroxo route (with H_2O_2).

In contrast, it is well known that oligomeric species shift the absorption edge to higher wavelengths,[20,21] as can be seen in Fig. 6e for Mo-MCM-41 synthesized without H_2O_2, following the oxo route.

Comparison of the spectra of samples freshly prepared (Fig. 6b) and after one month (Fig. 6c) shows that the absorption edge shifts towards higher wavelengths when samples are aged under normal atmosphere at room temperature. This indicates that crude products obtained with molybdenum consist mainly of low nuclearity oxo species which reorganize into oligomeric entities.

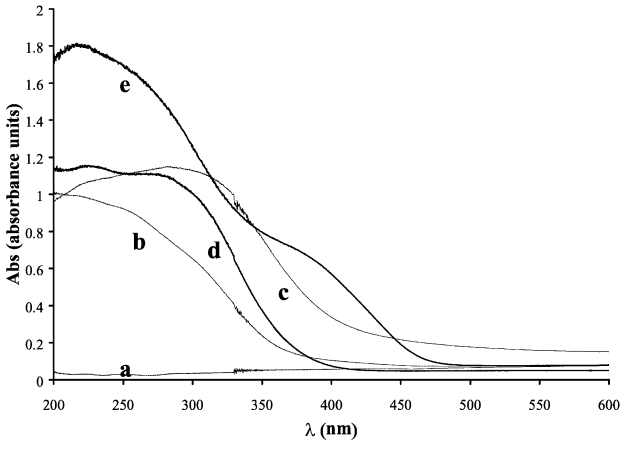

Fig. 6 UV-visible diffuse reflectance spectra of (a) SBA-15 all silica, (b) freshly prepared Mo-SBA-15 [$(Si/Mo)_{exp} = 46$], (c) Mo-SBA-15 after ageing one month [$(Si/Mo)_{exp} = 46$], (d) Mo-MCM-41 [peroxo route; $(Si/Mo)_{exp} = 35$] and (e) Mo-MCM-41 [oxo route; $(Si/Mo)_{exp} = 52$].

4. Conclusion

The peroxo route can easily be adapted from the synthesis of Mo-MCM-41[7] to develop molybdenum-containing SBA-15 mesoporous silica, Mo-SBA-15. Our data suggest that the molybdenum is inserted within the mesoporous framework with high metal dispersion. We are now investigating the incorporation of other peroxo metal centres such as tungsten(VI), rhenium(VII) or vanadium(V).

Work is in progress to evaluate the catalytic activity of these materials for oxidation processes involving oxidants like *t*-BuOOH or aqueous H_2O_2. Preliminary studies with such nucleophilic reagents have shown that molybdenum is leached out of the framework to a smaller or a larger extent; however, leaching of Mo from such materials is avoidable with non-polar reagents (gas/solid reactions or olefin metathesis under study).

Acknowledgements

We thank Dr. N. Lequeux (ESPCI/Paris) for XRD facilities and Dr. J. Lomas for correcting the manuscript.

References

1 G. Strukul, in *Catalytic Oxidations with Hydrogen Peroxide as Oxidant, Catalysis by Metals*, ed. G. Strukul, Kluwer Academic Publishers, Dordrecht, 1991, vol. 9, p. 177.
2 C. W. Jones, *Application of Hydrogen Peroxide and Derivatives, RSC Clean Technology Monographs*, The Royal Society of Chemistry, Cambridge, 1999.
3 T. Yanagisawa, T. Shimizu, K. Kuroda and C. Kato, *Bull. Chem. Soc. Jpn.*, 1990, **63**, 988.
4 C. T. Kresge, M. E. Leonowicz, J. W. Roth, J. C. Vartuli and J. S. Beck, *Nature*, 1992, **359**, 710.
5 J. S. Beck, J. C. Vartuli, W. J. Roth, M. E. Leonowicz, C. T. Kresge, K. D. Schmitt, C. T. W. Chu, D. H. Olson, E. W. Sheppard, S. B. McCullen, J. B. Higgins and J. L. Schlenker, *J. Am. Chem. Soc.*, 1992, **114**, 10 834.
6 E. Briot, J.-Y. Piquemal, M. Vennat, J.-M. Brégeault, G. Chottard and J.-M. Manoli, *J. Mater. Chem.*, 2000, **10**, 953.
7 J.-Y. Piquemal, J.-M. Manoli, P. Beaunier, A. Ensuque, P. Tougne, A.-P. Legrand and J.-M. Brégeault, *Microporous Mesoporous Mater.*, 1999, **29**, 291.
8 J.-Y. Piquemal, E. Briot, M. Vennat, J.-M. Brégeault, G. Chottard and J.-M. Manoli, *Chem. Commun.*, 1999, 1195.
9 J.-M. Brégeault, R. Thouvenot, S. Zoughebi, L. Salles, A. Atlamsani, E. Duprey, C. Aubry, F. Robert, and G. Chottard, in *Studies in Surface Science and Catalysis, New Developments in Selective Oxidation II*, ed. V. Cortès Corberàn and S. Vic Bellón, Elsevier, Amsterdam, 1994, vol. 82, p. 571.
10 L. Salles, C. Aubry, R. Thouvenot, F. Robert, C. Dorémieux-Morin, G. Chottard, H. Ledon, Y. Jeannin and J.-M. Brégeault, *Inorg. Chem.*, 1994, **33**, 871.
11 M. T. Pope, *Heteropoly- and Isopoly-oxometalates*, Springer-Verlag, Berlin, 1983.
12 J.-P. Jolivet, *De la Solution à l'Oxyde*, Inter Editions/CNRS Editions, Paris, 1994.

13 L. Karakonstantis, C. Kordulis and A. Lycourghiotis, *Langmuir*, 1992, **8**, 1318.
14 D. Zhao, J. Feng, Q. Huo, N. Melosh, G. H. Frederickson, B. F. Chmelka and G. D. Stucky, *Science*, 1998, **279**, 548.
15 D. Zhao, Q. Huo, J. Feng, B. F. Chmelka and G. D. Stucky, *J. Am. Chem. Soc.*, 1998, **120**, 6024.
16 W. Zhang, J. Wang, P. T. Tanev and T. J. Pinnavaia, *Chem. Commun.*, 1996, 979.
17 E. P. Barrett, L. G. Joyner and P. P. Halenda, *J. Am. Chem. Soc.*, 1951, **73**, 373.
18 M. Kruk, M. Jaroniec and A. Sayari, *Microporous Mater.*, 1997, **9**, 173.
19 M. Impéror-Clerc, P. Davidson and A. Davidson, *J. Am. Chem. Soc.*, 2000, **122**, 11 925.
20 R. S. Weber, *J. Catal.*, 1995, **151**, 470.
21 E. Iglesia, D. G. Barton, S. L. Soled, S. Miseo, J. E. Baumgartner, W. E. Gates, G. A. Fuentes, and G. D. Meitzner, in *Studies in Surface Science and Catalysis, 11th International Congress on Catalysis - 40th Anniversary*, ed. J. W. Hightower, W. N. Delgass, E. Iglesia and A. T. Bell, Elsevier, Amsterdam, 1996, vol. 101, p. 533.